

Constitutive modelling of knitted abdominal implants in numerical simulations of repaired hernia mechanics

Agnieszka Tomaszewska¹[0000-0001-5680-7979], Daniil Reznikov¹[0000-0001-5577-2057], Czesław Szymczak²[0000-0003-1989-5759] and Izabela Lubowiecka¹[0000-0003-0452-383X],

¹ Gdansk University of Technology, Faculty of Civil and Environmental Engineering
Narutowicza 11/12, 80-233 Gdansk, Poland
atomas@pg.edu.pl, danrezni.pg@gmail.com, lubow@pg.edu.pl

² Gdansk University of Technology, Faculty of Ocean Engineering and Ship Technology
Narutowicza 11/12, 80-233 Gdansk, Poland
szymcze@pg.edu.pl

Abstract. The paper presents a numerical approach to describe mechanical behavior of anisotropic textile material, which is a selected abdominal prosthesis. Two constitutive nonlinear concepts are compared. In the first one the material is considered composed from two families of threads (dense net model) and in the second one the material is homogeneous but anisotropic (as proposed by Gassel, Ogden, Holzapfel). Parameters of both models are identified based on experimental tensile tests (uni-axial and bi-axial, simple and cyclic). The constitutive relations are applied in numerical membrane model of the prosthesis applied in the abdominal wall. Its mechanical responses to the pressure loading has been compared, also to deflection experimentally observed in physical model of the operated hernia of the same geometry. The authors find that both constitutive models properly describe the implant's mechanics, but further studies are needed to possibly approach the outcome of hyperelastic anisotropic model to experimental results obtained for synthetic knit mesh.

Keywords: Hernia Repair, Abdominal Prosthesis, Mechanics, FEM Modelling, Experiment.

1 Introduction

Abdominal prostheses are applied to prevent hernia occurrence in post-operational scar or to reconstruct abdominal wall in a case of hernia so that its structural function is restored. As typical in the human body reparation, hernia management deals with searching for the best solutions [1]. In a number of cases the operation is followed by permanent pain or even by the sickness recurrence [2], [3]. The hernia recurrence is observed when the implant fixation device is overloaded and the prosthesis is disconnected with the abdominal tissue. The load bearing capacity of selected tacks and sutures has been described e. g. in [4]. Proper hernia management depends on an accurate to a given case selection of the implant and its fixation. Many medical papers discuss that problem, also other than medical studies are undertaken to understand the

biology and mechanics of operated abdominal hernia. They cover experiments on animals, in which tissue-mesh incorporation is observed [5], [6], *ex-vivo* experiments on operated hernia models with the use of animal tissue [7], [8], [9] experiments on living human abdominal wall to recognize its mechanical properties [10], [11], [12], mechanical tests of abdominal prostheses to observe their behavior and to identify their mathematical models [13], [14], [15] and finally, many numerical studies and simulations [16], [17], [18], [19].

In the present paper numerical modelling of the prosthesis implanted in the abdominal wall is considered. The study refers to DynaMesh[®]-IPOM mesh. Finite Elements Method (FEM) is applied. The study is focused on constitutive modelling of the prosthesis. Two different concepts are compared. In the first one the mesh is modelled as a woven textile comprising two families of threads with non-linear stress-strain relation. Dense net material model is applied here [20]. In the second one the material is modelled with the use of homogeneous hyperelastic anisotropic material model, as proposed in [21]. That model is defined rather for tissues but the authors were tempted to analyze its suitability for modeling the implant as its knit wear structure can be treated as fibrous. The model was already applied in similar sense as it is described in [22].

In both cases the model is loaded by ‘intra-abdominal’ pressure, the deflection is calculated and compared to experimentally measured on corresponding physical model (experimental results are described in [23]).

2 Materials and methods

2.1 The implant

DynaMesh[®]-IPOM (FEG Textiltechnik GmbH, Aachen, Germany) is selected. It is a synthetic knit mesh, in which polypropylene (PP) filaments (12%, placed on parietal side) are interlinked with polyvinylidene fluoride (PVDF) threads (88%, placed on visceral side).

2.2 Constitutive models

Dense net constitutive model. This model is dedicated for woven materials [24], [25]. It has been applied in static and dynamic analysis performed for designing structures built with the use of textile material, e. g. Forest Opera in Sopot (Poland). In the authors team it serves for modelling textile, reticular or knitted implants. In this concept woven material is treated as a continuum without explicit reference to its discrete microstructure. Two directions $\xi \in (1,2)$ in the structure plane are distinguished and it is assumed that cross-sectional membrane forces T in the two directions ξ depend solely on the uniaxial strains in these directions $(\varepsilon_1, \varepsilon_2)$. Thus, the following constitutive equation is postulated:

$$\mathbf{T}_\xi = \begin{Bmatrix} T_1 \\ T_2 \end{Bmatrix} = \begin{bmatrix} F_1 & 0 \\ 0 & F_2 \end{bmatrix} \begin{Bmatrix} \varepsilon_1 \\ \varepsilon_2 \end{Bmatrix}, \quad (1)$$

where F_1 and F_2 denote the material's tension stiffness in the two selected directions (1,2). The details of the model can be found e.g., in [20] where it was defined and, in [16] where it was applied in implant modelling, in [23] where some mechanical analyses with this model were undertaken. In this study this stiffness is identified based on uni-axial tension tests that is possible due to the model specifics as mentioned before.

Hyperelastic anisotropic model. The anisotropic hyperelastic model is described using the Gasser-Ogden-Holzapfel (GOH) model [26]. The strain energy density function (SEDF) for this model is expressed as:

$$\Psi = C_{10}(I_1 - 3) + \sum_{i=4,6} \frac{k_1}{2k_2} (e^{k_2(\kappa I_i + (1-3\kappa)I_i - 1)^2} - 1), \quad (2)$$

where C_{10} and k_1 are stress – like parameters, k_2 – is a dimensionless parameter and κ describes the dispersion of the fibers. The SEDF contains two parts. The first term describes an isotropic behavior of the material (the influence of the matrix material) and the second term describes an anisotropic behavior of the material (the contribution of collagen fibers). I_1 is the first invariant of the Cauchy-Green tensor $\mathbf{C} = \mathbf{F}^T \mathbf{F}$.

$$I_1 = \text{tr}(\mathbf{C}) \quad (3)$$

The terms I_4 and I_6 are two pseudo – invariants of \mathbf{C} . They describe the properties of the fiber family

$$I_4 = \mathbf{a}_0 \cdot \mathbf{C} \mathbf{a}_0, \quad I_6 = \mathbf{g}_0 \cdot \mathbf{C} \mathbf{g}_0. \quad (4)$$

$$\mathbf{a}_0 = \begin{bmatrix} \cos(\alpha) \\ \sin(\alpha) \\ 0 \end{bmatrix}, \quad \mathbf{g}_0 = \begin{bmatrix} \cos(\alpha) \\ -\sin(\alpha) \\ 0 \end{bmatrix} \quad (5)$$

where \mathbf{a}_0 and \mathbf{g}_0 are the unit vectors which describe the directions of fibers in the undeformed configuration [27]. The second Piola – Kirchoff stress can be calculated as:

$$\mathbf{S} = -p\mathbf{C}^{-1} + 2 \frac{\partial \Psi(\mathbf{C})}{\partial \mathbf{C}} \quad (6)$$

where p is the Lagrangian multiplier. Parameters of the model are identified based on biaxial tensile tests of DynaMesh-IPOM samples.

2.3 Description of the experiments

Simple tension tests. Rectangular samples cut in two orthogonal directions of the material have been prepared and subjected to tests. The directions specified are parallel (direction 1) and perpendicular (direction 2) to the mesh knitting pattern. The samples of the width of 30 mm have been subjected to failure tension tests and to cyclic loading experiments, with various force ranges, between 0.5 and 2-20 N. Zwick Roel Z020 machine with videoextensometer has been utilized. The details of the experiments are presented in [13].

Biaxial tension tests. Square sample of DynaMesh-IPOM has been prepared. Its edges are parallel to the knitting pattern of the mesh. It has been placed on Biax Zwick Roel machine using specially constructed rakes. The square field of the material, with side dimension of 50mm has been subjected to biaxial tension tests. From uniaxial tests it is known that the mesh reveals orthotropic properties – ratio of elastic moduli determined for two orthogonal directions is approximately 4.5. Thus, the following various force ratios have been applied in the tests: 1:1, 1:2, 1:1.5. Bigger force has been applied in the stiffer direction of the mesh. Maximal force applied equals 12 N. The experimental set up is shown in Fig. 1. To identify Cauchy-Green deformation tensor 2-camera Digital Image Correlation system has been used. The system tracks positions of four markers placed on the sample (see Fig. 1).



Fig. 1. Set up in biaxial tests

2.4 Numerical models and simulation

The models geometry responses to physical model of operated ventral hernia built of a porcine abdominal wall and DynaMesh-IPOM, which has been subjected to cyclic pressure loading (simulation of post-operational cough). The details of the experimental setup and the results are described in the paper [23].

In the numerical modelling the implant is represented by membrane finite elements with four nodes and three translational degrees of freedom in each node. The structure is circular, with a diameter of 13.5 cm. It is supported in 19 points evenly distributed on the circumference. In the central circular region, with a diameter of 7 cm, hernia orifice is supposed so this region is built only of the membrane (prosthesis). The ring around that hernia orifice is the overlap of the implant and the abdominal wall. It is modelled by a membrane (prosthesis) supported by elastic foundation (abdominal wall). Such set up is sufficient for the action simulated, which is pressure loading. The stiffness of the elastic foundation is 2.7 MPa, as identified in earlier study [16]. The pressure is applied as in the experiment, linearly growing from 0 to 7.75 kPa within 4s.

Two FEM models created in commercial software are compared here. The first one, *M1* model, built in the MSC.Marc is described in details in [23]. It is supplemented by linear springs placed radially in the supporting points in the model plane. The springs mimic the abdominal wall elasticity, their stiffness coefficient is 1500 N/m. Dense net material model is applied in this case. Dynamic analysis is performed here with damping coefficients as described in [16]. The second, *M2* model, is made in Abaqus. Hyperelastic anisotropic material model is applied here. Nonlinear static analysis is performed with an increment size 0.05. Due to the numerical instabilities that may occur in membranes analysis both models demand initial tension, as discussed in [28]. In the model *M1* the initial stress is applied directly to the elements while in the model *M2* it is achieved by initial displacements of the model supports.

3 Results

3.1 Parameters of the constitutive models

The models are identified with the use of Marquardt–Levenberg variant of the least squares method. Compatibility of the hyperelastic anisotropic model with the experimental data is shown in Fig. 2. The data come from fifth in a row test of biaxial tension, so the sample is in the preconditioned state. The applied force ratio in two directions is 1:1.5. Force value of 12 N is applied in the stiffer direction of the material. The fitting accuracy is acceptable, as the correlation coefficients are 0.9982 and 0.9838 for two curves considered. The parameters of the model are placed in Table 1.

Table 1. Parameters of hyperelastic anisotropic model of DynaMesh-IPOM

Parameter	C_{10} [MPa]	k_1 [MPa]	k_2 [-]	κ [-]	α [rad]
Value	1.3005	2.8813	50.3756	0.0188	0.5170

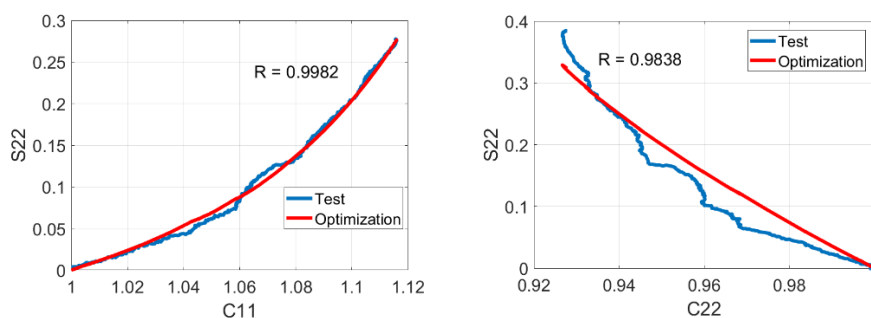


Fig. 2. Results of the hyperelastic model identification

Based on the uni-axial tests the DynaMesh-IPOM stiffness function necessary in dense net model in the two directions has been specified by determining elastic modulus values for each loading path. Baseline (based on failure tension tests) and precon-

ditioned (based on cyclic loading tests) states of the material have been described. Identification details are described in [23]. Here the elastic moduli values, which form piecewise constant stiffness functions in the two distinguished directions of the prosthesis in the preconditioned state are considered. They are shown in Table 2.

Table 2. Parameters of stiffness functions in dense net model

Strain range, direction 1	Elastic modulus value [N/m]	Strain range, direction 2	Elastic modulus value [N/m]
0.00-0.10	594.00	0.00-0.06	1678.00
0.10-0.20	824.00	0.006-0.13	2650.00
0.20-0.25	1130.00	0.13-0.18	3850.00
0.25-0.35	1603.00	0.18-0.22	5700.00
0.35-0.45	2520.00	0.22-0.28	10650.00
0.45-0.55	4000.00		
0.55-0.65	6000.00		

3.2 Numerical simulations results

Maximum principal stress distribution calculated in the models *M1* and *M2* are presented in Fig. 3. The maximum value of the reaction force is obtained in the direction *x* in *M1* model (the values is 1.42 N) and in the direction *y* in *M2* model (with the value of 3.01 N). The deflection value experimentally observed equals 17 mm (as described in [23]). The value calculated in *M1* model is 16 mm and in the *M2* model it is 8 mm.

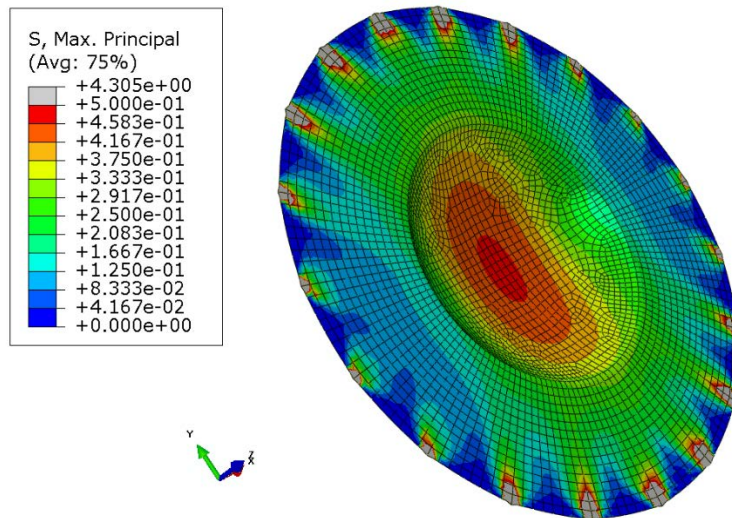
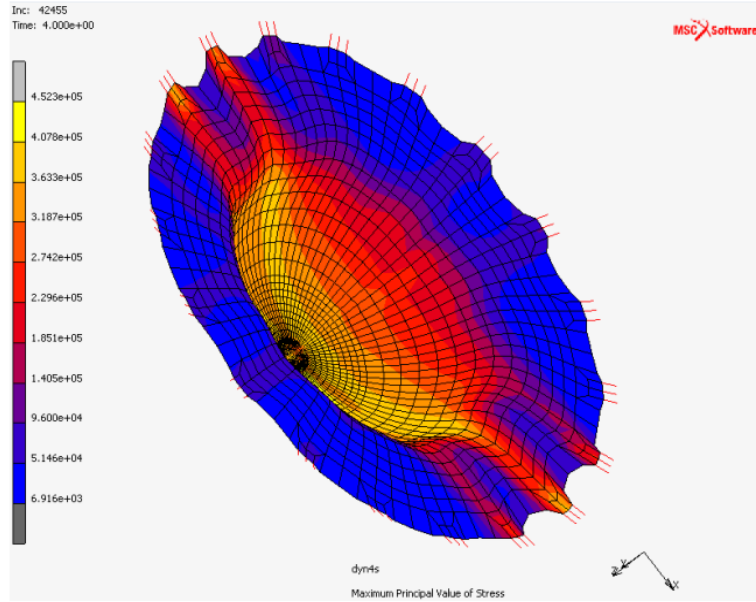


Fig. 3. Maximum principal stress calculated in *M1* model in [Pa] (the upper one) and in *M2* model in [MPa] (the bottom one)

4 Discussion and conclusion

The two numerical models reveal similar response to the pressure loading. Zone of increased stress is observed in the direction of bigger stiffness of the material. Maximum stress value in both models equals 4.5 MPa approximately. However, the deflection calculated in the *M2* model is twice smaller than in the *M1* model and the maximum reaction in *M2* model is twice bigger than in *M1* model. Such relation between deflection and reaction in supporting points is typical in membrane and cable models (see e. g. [29]). The results obtained may suggest that an application of GOH constitutive relation makes the model more stiff than an application of dense net material model. But both numerical models have been created differently. The *M1* model has been validated to the experiment on hernia model, which is described in [23] and the deflection calculated in it responses to the physically measured. The *M2* model has been built based on parameters of *M1* model, including boundary conditions. The difference between outcome of the two models suggest that *M2* model should be validated to the experiment separately.

The aim of the study was to compare the effectiveness of two different constitutive concepts in application to a selected abdominal prosthesis, which is an anisotropic textile material. The authors have a well-established experience in the dense net model application in the cases of this kind. However, other groups apply hyperelastic anisotropic model to mimic mechanical behavior of such meshes (see e. g. [22]). In general both models reveal similar response to the load applied. However, by comparison of the results concerning deflection obtained in the two models one may hold a preliminary opinion that dense net material model describes the prosthesis behavior better than the homogeneous one. Further research aiming at obtaining bigger similarity between *M1* and *M2* models are needed, e. g. stiffness functions for dense net model should be identified from biaxial tests, the same as used in GOH model, *M2* model should be validated separately to the experiments to determine boundary conditions.

Acknowledgments

This work has been partially supported by the National Science Centre (Poland) [grant No. UMO-2017/27/B/ST8/02518]. Calculations have been carried out at the Academic Computer Centre in Gdansk.

References

1. Pawlak M., Bury K., Śmietański M.: The management of abdominal wall hernias - in search of consensus. Videosurgery other miniinvasive Tech. / Kwart. Pod patronatem Sekc. Wideochirurgii TChP oraz Sekc. Chir. Bariatrycznej TChP, vol. 10, no. 1, pp. 49–56, Apr. 2015.
2. Sauerland S., Walgenbach M., Habermalz B., Cm S, Miserez M.: Laparoscopic versus open surgical techniques for ventral or incisional hernia repair (Review).Cochrane Libr., no. 3, pp. 1–62, 2011.

3. Bansal V.K., Misra M.C., Kumar S., Rao Y.K., Singhal P., Goswami A., Guleria S., Arora M. K., Chabra A.: A prospective randomized study comparing suture mesh fixation versus tacker mesh fixation for laparoscopic repair of incisional and ventral hernias. *Surg. Endosc.*, vol. 25, no. 5, pp. 1431–8, May 2011.
4. Tomaszewska A., Lubowiecka I., Szymczak C., Smietański M., Meronk B., Kłosowski P., Bury K.: Physical and mathematical modelling of implant-fascia system in order to improve laparoscopic repair of ventral hernia. *Clin. Biomech. (Bristol, Avon)*, vol. 28, no. 7, pp. 743–51, Aug. 2013.
5. Anurov M.V., Titkova S. M., Oettinger P.: Biomechanical compatibility of surgical mesh and fascia being reinforced: dependence of experimental hernia defect repair results on anisotropic surgical mesh positioning. *Hernia*, vol. 16, no. 2, pp. 199–210, Apr. 2012.
6. Gomez-Gil V., Rodriguez M., Garcia-Moreno Nisa F., Perez-Kohler B., Pascual G.: Evaluation of synthetic reticular hybrid meshes designed for intraperitoneal abdominal wall repair : Preclinical and in vitro behavior. *PLoS One*, vol. 14, no. 2, pp. 1–26, 2019.
7. Podwojewski F., Otténio M., Beillas P., Guérin G., Turquier F., Mitton D.: Mechanical response of human abdominal walls ex vivo: Effect of an incisional hernia and a mesh repair. *J. Mech. Behav. Biomed. Mater.*, vol. 38, pp. 126–33, Oct. 2014.
8. Röhrnbauer B., Ozog Y., Egger J., Werbrouck E., Deprest J., Mazza E.: Combined biaxial and uniaxial mechanical characterization of prosthetic meshes in a rabbit model. *J. Biomech.*, vol. 46, no. 10, pp. 1626–32, Jun. 2013.
9. Kallinowski F., Gutjahr D., Vollmer M., Harder F., Nessel R.: Increasing hernia size requires higher GRIP values for a biomechanically stable ventral hernia repair. *Ann. Med. Surg.*, 2019.
10. Song C., Alijani A., Frank T., Hanna G., Cuschieri A.: Elasticity of the living abdominal wall in laparoscopic surgery. *J. Biomech.*, vol. 39, no. 3, pp. 587–91, Jan. 2006.
11. Todros S., de Cesare N., Pianigiani S., Concheri G., Savio G., Natali A. N., Pavan P. G.: 3D Surface Imaging of Abdominal Wall Muscular Contraction Silvia. *Comput. Methods Programs Biomed.*, 2019.
12. Szymczak C., Lubowiecka I., Tomaszewska A., Smietański M.: Investigation of abdomen surface deformation due to life excitation: implications for implant selection and orientation in laparoscopic ventral hernia repair. *Clin. Biomech. (Bristol, Avon)*, vol. 27, no. 2, pp. 105–10, Feb. 2012.
13. Tomaszewska A.: Mechanical behavior of knit synthetic mesh used in hernia surgery. *Acta Bioeng. Biomech.*, vol. 18, no. 1, pp. 77–86, 2016.
14. Deeken C. R., Thompson D. M., Castile R. M., Lake S. P.: Biaxial analysis of synthetic scaffolds for hernia repair demonstrates variability in mechanical anisotropy, non-linearity and hysteresis. *J. Mech. Behav. Biomed. Mater.*, vol. 38, pp. 6–16, Oct. 2014.
15. Röhrnbauer B., Mazza E.: Uniaxial and biaxial mechanical characterization of a prosthetic mesh at different length scales. *J. Mech. Behav. Biomed. Mater.*, vol. 29, pp. 7–19, Jan. 2014.
16. Lubowiecka I.: Mathematical modelling of implant in an operated hernia for estimation of the repair persistence. *Comput. Methods Biomech. Biomed. Engin.*, Jun. 2013.
17. Lubowiecka I., Szepietowska K., Szymczak C., Tomaszewska A.: A PRELIMINARY STUDY ON THE OPTIMAL CHOICE OF AN IMPLANT. *J. Theor. Appl. Mech.*, vol. 53, no. 2, pp. 411–421, 2016.
18. Pavan P. G., Todros S., Pachera P., Pianigiani S., Arturo N.: Engineering The effects of the muscular contraction on the abdominal biomechanics : a numerical investigation a numerical investigation. *Comput. Methods Biomech. Biomed. Engin.*, vol. 22, no. 2, pp. 139–148, 2019.



19. Simón-Allué R., Hernández-Gascón B., Lèoty L., Bellón J. M., Peña E., Calvo B.: Prostheses size dependency of the mechanical response of the herniated human abdomen. *Hernia*, Aug. 2016.
20. Branicki C., Kłosowski P.: Statical analysis of hanging textile membranes in nonlinear approach. *Arch. Civ. Eng.*, vol. XXIX, no. 3, pp. 189–219, 1983.
21. Holzapfel G. A., Gasser T. C., Ogden R.W.: A New Constitutive Framework for Arterial Wall Mechanics and a Comparative Study of Material Models. *J. Elast.*, vol. 61, pp. 1–48, 2000.
22. Hernández-Gascón B., Peña E., Grasa J., Pascual G., Bellón J. M., Calvo B.: Mechanical Response of the Herniated Human Abdomen to the Placement of Different Prostheses. *J. Biomech. Eng.*, vol. 135, no. 5, p. 051004, Apr. 2013.
23. Tomaszewska A., Lubowiecka I., Szymczak C.: Mechanics of mesh implanted into abdominal wall under repetitive load. Experimental and numerical study. *J. Biomed. Mater. Res. Part B Appl. Biomater.*, vol. 107, no. 5, pp. 1400–1409, 2019.
24. Ambroziak A., Kłosowski P.: Review of constitutive models for technical woven fabrics in finite element analysis. *AATCC Rev.*, vol. 11, no. 3, pp. 58–67, 2011.
25. Kłosowski P., Zerdzicki K., Woznica K.: Identification of Bodner-Partom model parameters for technical fabrics. *Comput. Struct.*, vol. 187, no. 187, pp. 114–121, 2017.
26. Gasser T. C., Ogden R. W., Holzapfel G. A.: Hyperplastic modeling of arterial layers with distributed collagen fiber orientations. *J. R. Soc. Interface*, vol. 3, no. September 2005, pp. 15–35, 2006.
27. Holzapfel G.: *Nonlinear solid mechanics. A Continuum Approach for Engineering*. New York: John Wiley & Sons, 2000.
28. Lubowiecka I., Szymczak C., Tomaszewska A., Śmietański M.: A FEM membrane model of human fascia – synthetic implant system in a case of a stiff ventral hernia orifice. *Shell Structures. Theory and Applications*, 2010, pp. 311–314.
29. Szymczak C., Lubowiecka I., Tomaszewska A., Śmietański M.: Modeling of the fascia-mesh system and sensitivity analysis of a junction force after a laparoscopic ventral hernia repair. *J. Theoretical Appl. Mech.*, vol. 48, no. 4, pp. 933–950, 2010.

